Liquid Crystals
Publication details, including instructions for authors and subscription information:
http://www.informaworld.com/smpp/title~content=t713926090

Studies of the higher order smectic phase of the large electroclinic effect material W317

P. A. Williams[ab]; L. Komitov[c]; A. G. Rappaport[a]; B. N. Thomas[ad]; N. A. Clark[a]; D. M. Walba[e]; G. W. Day[b]

[a] Department of Physics, Condensed Matter Laboratory, University of Colorado, Boulder, Colorado, U.S.A. [b] National Institute of Standards and Technology, Boulder, Colorado, U.S.A. [c] Chalmers University of Technology, Göteborg, Sweden [d] Exxon Research and Eigineering, Annandale, New Jersey, U.S.A. [e] Department of Chemistry and Biochemistry and Optoleectronic Computing Systems Center, University of Colorado, Boulder, Colorado, U.S.A.

To cite this Article Williams, P. A. , Komitov, L. , Rappaport, A. G. , Thomas, B. N. , Clark, N. A. , Walba, D. M. and Day, G. W.(1993) 'Studies of the higher order smectic phase of the large electroclinic effect material W317', Liquid Crystals, 14: 4, 1095 — 1105
To link to this Article: DOI: 10.1080/02678299308027818
URL: http://dx.doi.org/10.1080/02678299308027818

LIQUID CRYSTALS, 1993, VOL. 14, NO. 4, 1095–1105

Studies of the higher order smectic phase of the large electroclinic effect material W317

by P. A. WILLIAMS*†‡, L. KOMITOV§, A. G. RAPPAPORT†, B. N. THOMAS†¶, N. A. CLARK†, D. M. WALBA‖ and G. W. DAY‡

† Department of Physics, Condensed Matter Laboratory, University of Colorado, Boulder, Colorado 80309-0390, U.S.A.

‡ National Institute of Standards and Technology, Boulder, Colorado 80303-3328, U.S.A.

§ Chalmers University of Technology, S-412 96 Göteborg, Sweden

¶ Exxon Research and Eigineering, Route 22 East, Annandale, New Jersey 08801, U.S.A.

‖ Department of Chemistry and Biochemistry and Optoleectronic Computing Systems Center, University of Colorado, Boulder, Colorado 80309-0215, U.S.A.

We present studies of the large electroclinic effect material W317. We found via X-ray scattering, calorimetry and optical observation that quenching from the smectic A* phase results in several higher order phases including an orthogonal (hexatic) smectic with short range in-layer translational order and no interlayer order. We characterize the electroclinic response in the quenched phase, and determine its magnitude and response time as a function of electric field amplitude and temperature.

1. Introduction

The new liquid crystal material W317 [1] has the largest electroclinic effect reported [2], with tilt angles $>20°$ easily achievable (see figure 1). The electroclinic effect in W317 is also unusually stable with temperature (see figure 2) which is a further advantage over other materials with relatively large electroclinic effects [3–5]. We have found that at least three metastable orthogonal phases lie below the smectic A* phase of W317. In this paper, we discuss the nature and ramifications of these phases, and characterize their electroclinic response.

2. Underlying orthogonal phases

The molecular structure of W317 is

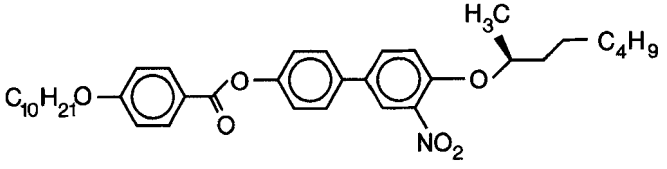

and its phase sequence is

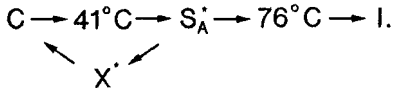

* Author for correspondence.

0267–8292/93 $10·00

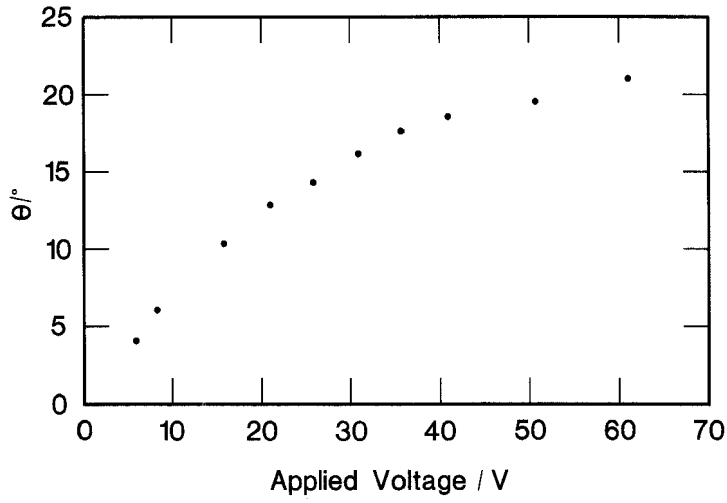

Figure 1. Electronic tilt angle versus voltage ($\sim 2{\cdot}1$ μm cell) in the smectic A* phase, $T = 27{\cdot}1$°C.

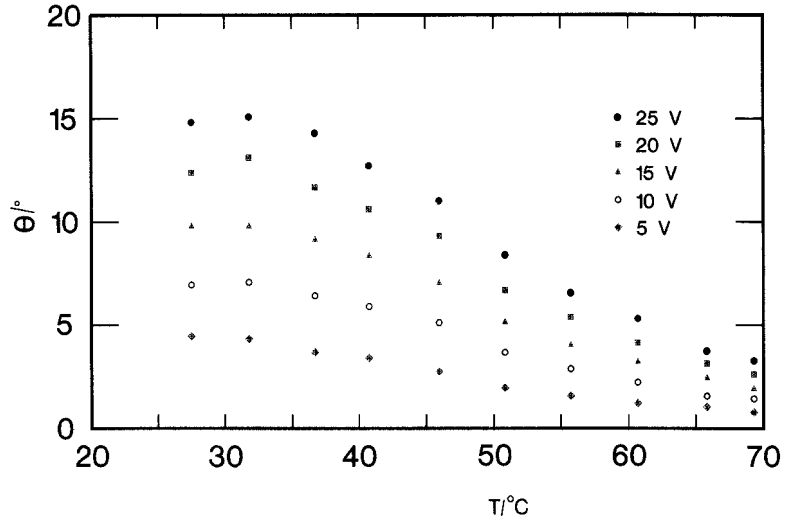

Figure 2. Electroclinic tilt angle versus temperature for various voltages, all data taken in the smectic A* phase for a $\sim 2{\cdot}1$ μm cell.

Above 41°C, the smectic A* phase is stable. However, W317 can be supercooled below 41°C and remain in the smectic A* phase for several hours before crystallizing. If the smectic A* phase is cooled rapidly enough, metastable higher order phases can be reached at ~ 0°C. The metastability of these phases prevents the assignment of definite temperature ranges. Although we have investigated this phase behaviour by optical observation, differential scanning calorimetry (DSC) and X-ray scattering, we have not yet identified these phases. Therefore, for now, we denote them collectively as X* phases.

X-ray scattering yielded the most detailed picture of the low temperature phase behaviour. The wavelength of our X-ray source was 0·9494 Å. We performed X-ray scattering measurements on a capillary sample of W317 as it was quenched to about

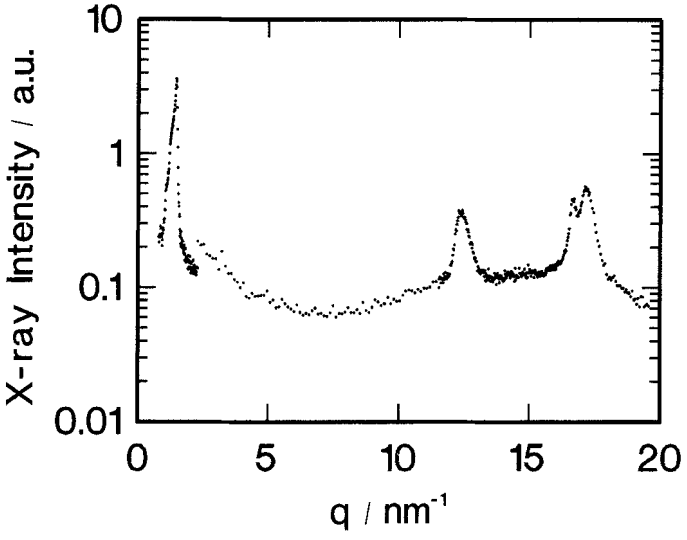

Figure 3. X-ray scattering intensity versus scattering vector in the first higher order phase to appear (a smectic with in-layer order).

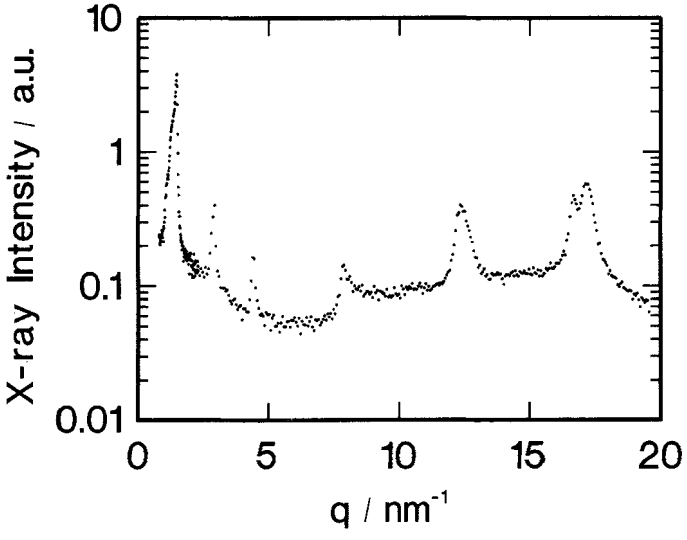

Figure 4. X-ray scattering intensity versus scattering vector; higher order layer peaks appear.

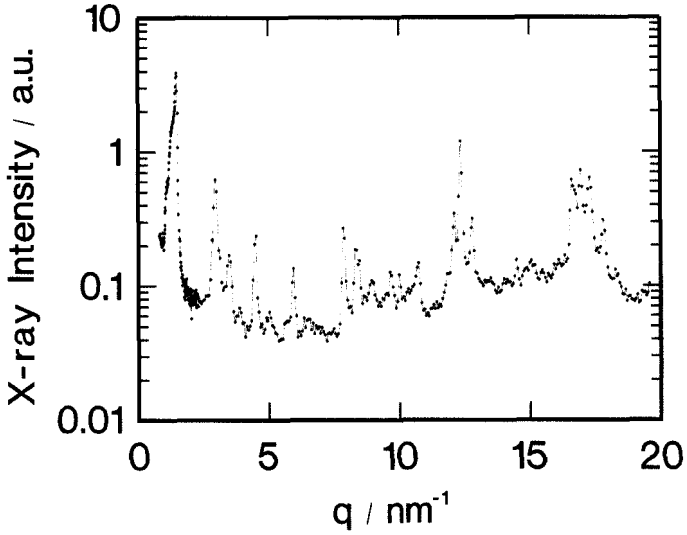

Figure 5. X-ray scattering intensity versus scattering vector; crystal structure.

-5°C from the smectic A* phase. We found at least three separate phases below the smectic A* phase. However, the transition temperatures of these phases and the length of time they lasted (sometimes, they did not appear at all) depended on the quenching rate. Heating the sample to ~ 35°C brought back the smectic A* phase. Figures 3, 4, and 5 are plots of X-ray intensity versus the scattering vector **q**, illustrating the three higher order phases in the order they appeared during heating from a particular quench. The first phase to appear was a smectic with in-layer translational ordering, but no interlayer order (see figure 3). In the second phase (see figure 4), the layers have sharpened, but there is no change of the in-layer ordering. In the third phase (see figure 5), a transition has been made to a complicated crystal structure. We have not yet been able to match these X-ray scattering results to any known phases. The two broad in-layer peaks of figures 3–5 do not seem to agree with a simple E* or B* identification.

We also observed these three higher order phases using differential scanning calorimetry. As already mentioned, the transition temperatures of these phases are dependent on cooling rate. Figures 6 and 7 show results for one particular temperature cycle. A sample of W317 was cooled from 80°C to -20°C at a rate of 1°C min^{-1}, and then heated back to 80°C at the same rate. Figures 6 and 7 show the heat flow into the sample versus temperature during the cooling and heating processes. In these figures, heat flowing into the sample is positive. Therefore, a dip in the curve indicates a transition to a lower energy (higher order) phase. In figure 6, W317 is cooled from the isotropic phase. The sharp dip at ~ 73°C indicates the heat given off by the sample as it enters the smectic A* phase. As the sample is further cooled, it makes two broad transitions into higher order phases at approximately 10°C and -10°C. As the sample is heated (see figure 7), a transition to a third higher order phase is seen at ~ 15°C. Then, the transition into the smectic A* phase starts at ~ 35°C. Finally, the isotropic phase is again reached at ~ 73°C.

We also observed the smectic A*–X* transition using polarizing microscopy. Through the microscope, we located a focal-conic domain in the smectic A* phase. In such a domain, the layers form concentric circles, with the molecules lying along radii

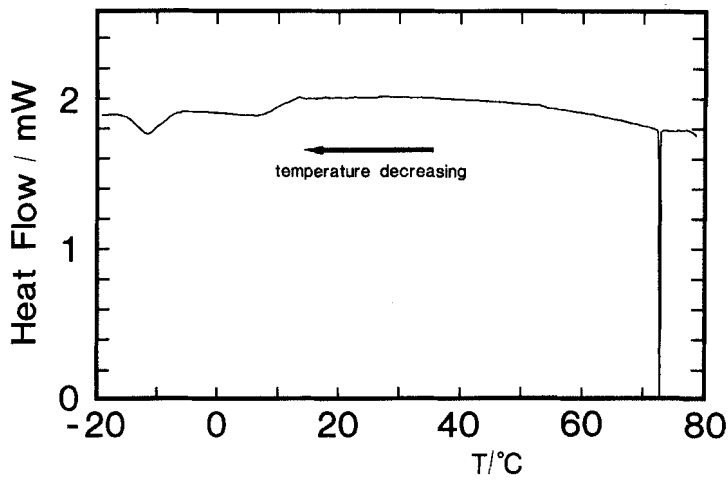

Figure 6. Heat flow into sample versus temperature as sample was cooled from 80°C to −20°C.

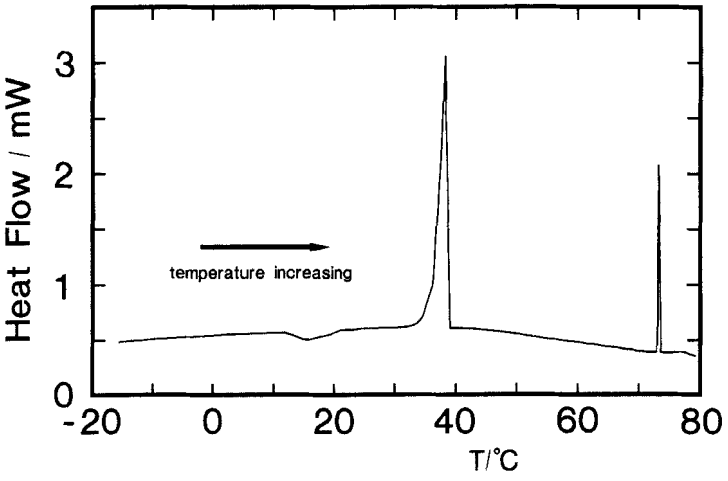

Figure 7. Heat flow into sample versus temperature as sample was heated from −20°C to 80°C.

from the centre of this region. This gives a cross-shaped brush pattern when viewed between crossed polarizers (see figure 8 (*a*)). As we cooled the sample through the smectic A*–X* transition, we saw no rotation of this cross (see figure 8 (*b*)). We conclude that in these higher order phases, the molecules are still normal to the layers. We have also observed optically lines running parallel to the layer direction in the X* phases (evidence of an E* phase). However, a simple E* identification disagrees with X-ray results.

3. Experimental set-up

We measured the electroclinic tilt angles and response times using the set-up of figure 9. Liquid crystal cells were aligned between rubbed nylon-coated glass slides. This gave a planar alignment with the molecules parallel to the glass slides. Two

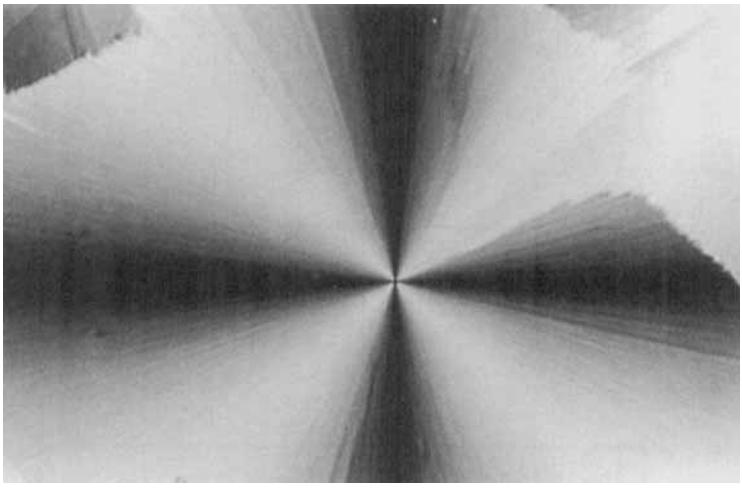

(*a*)

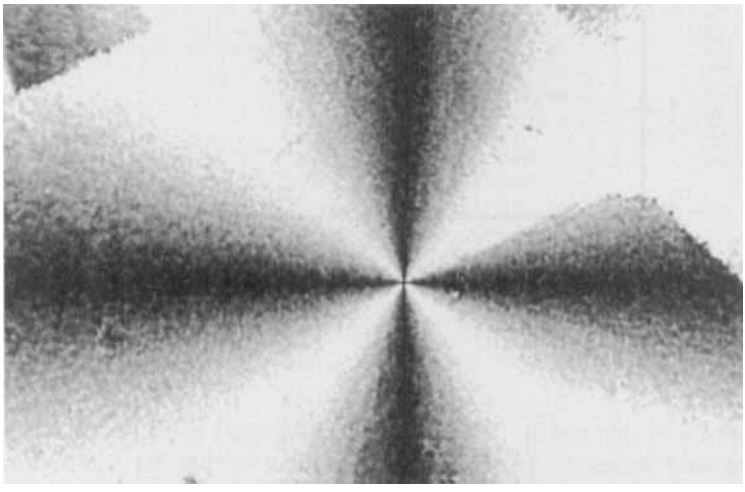

(*b*)

Figure 8. Focal-conic texture viewed between crossed polarizers. There is no rotation of the cross as the sample goes from (*a*) the smectic A* phase at $T = 31°C$ to (*b*) the smectic X* phase at $T = -3°C$.

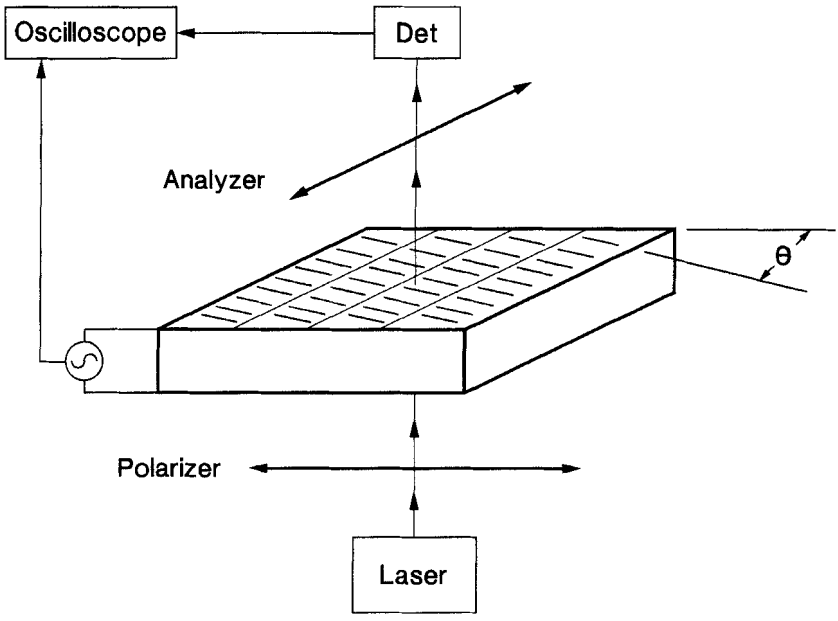

Figure 9. Experimental orientation of the liquid crystal cell between crossed polarizers.

different cells were used in these measurements, one of thickness $\sim 3{\cdot}6\,\mu$m, and the other, a $\sim 2{\cdot}1\,\mu$m cell, was shear aligned to produce better alignment. Transparent indium tin oxide (ITO) layers on each slide were used as electrodes to give an electric field perpendicular to the slides and parallel to the smectic layers. For the experiment, the cell was held in a temperature controlled heater, placed between crossed polarizers and rotated so that the molecular axis made a 22·5° angle with one of the polarizers to maximize the optical response.

To measure the electroclinic tilt angle, a sinusoidal voltage was applied to the cell, causing the liquid crystal molecules to tilt back and forth in the plane of the cell. This modulation of the liquid crystal director caused a corresponding modulation of the detected intensity of a laser beam passing through the polarizer–cell–analyser combination. This give an optical intensity proportional to $\sin^2\{2(22{\cdot}5° + \theta)\}$ or $(1 + \sin 4\theta)$, where θ is the electroclinic tilt angle [5]. The optical response was then inverted to find the value of θ which resulted from a given voltage. For the data of figure 1, an applied DC voltage was used in place of an AC voltage. To measure the electroclinic response time, we applied a square wave voltage to the cell, and measured the 10–90 per cent rise time of the optical signal.

4. Electroclinic measurements

In order to measure the electroclinic effect in the lower temperature X* phases, we cooled the sample rapidly ($\sim 2°\text{C min}^{-1}$) until we observed a phase transition from the smectic A* phase. We identified the phase transition optically and by observing a drop in the size of the electroclinic effect.

Plots of electroclinic tilt angle θ versus voltage for several temperatures (in the X* phases) are shown in figure 10. There is still a linear electroclinic effect in the X* phases which yields large tilt angles. However, the magnitude of the electroclinic coefficient is

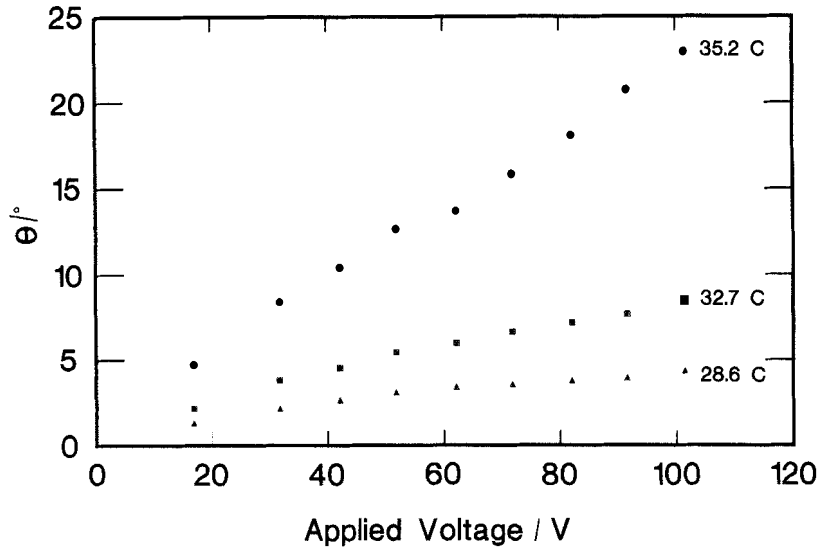

Figure 10. Electroclinic tilt angle versus voltage (~2·1 μm cell) for various temperatures, all in the X* phases.

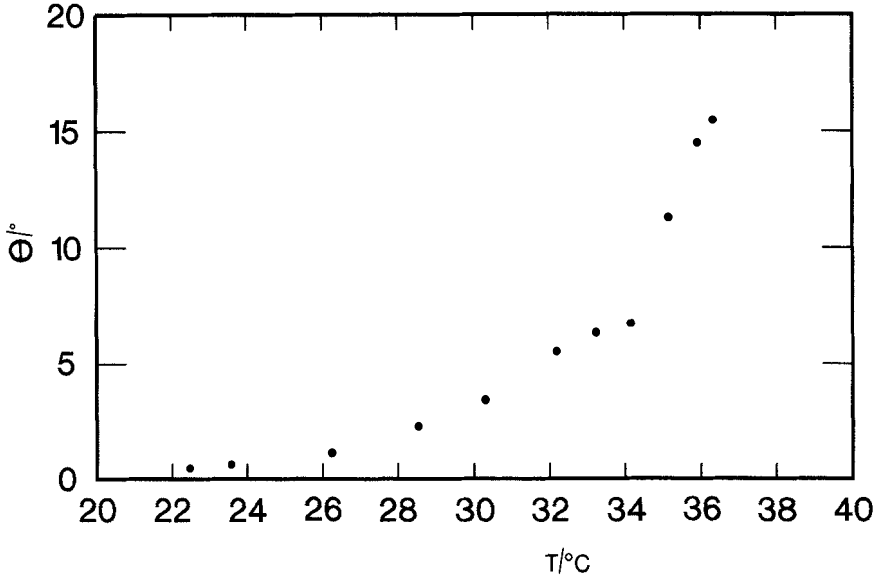

Figure 11. Electroclinic tilt angle versus temperature in the X* phase from an applied voltage of 100 V (~2·1 μm cell).

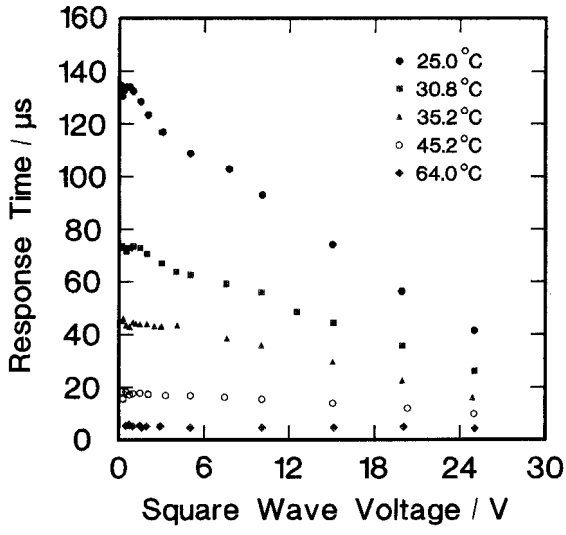

Figure 12. 10–90 per cent response time versus voltage (~3·6 μm cell) for various temperatures in the smectic A* phase.

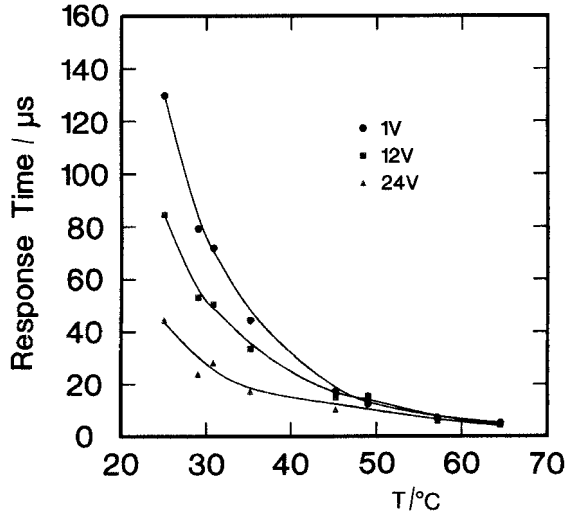

Figure 13. 10–90 per cent response time versus temperature for various voltages (~3·6 μm cell) in the smectic A* phase.

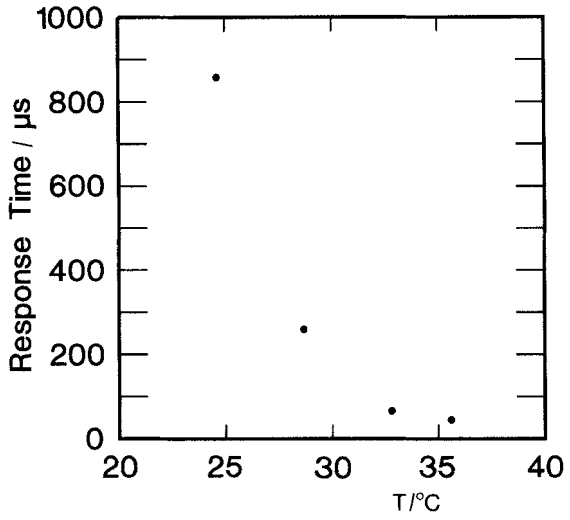

Figure 14. 10–90 per cent response time versus temperature in the X* phases for an applied voltage of 180 V (~2·1 μm cell).

reduced from its value in the smectic A* phase. We also measured the temperature dependence of the electroclinic effect in the X* phases (see figure 11). However, these temperature data are only qualitative, since the metastability of the phase made the results difficult to repeat.

Figures 12, 13 and 14 show the response time of the electroclinic effect in both the smectic A* and X* phases as a function of temperature and voltage. In the smectic A* phase, response times are dependent on voltage at low temperatures and approach a small voltage-independent value at higher temperatures (see figures 12 and 13). This is qualitatively the behaviour expected for a large tilt electroclinic material [6, 7]. However, the smectic A* phase response times of W317 range from ~5 μs to ~140 μs which is slower than for most reported electroclinic materials [3, 8–10]. In the X* phase, the response times are even slower, but speed up at higher temperatures (see figure 14).

5. Discussion

The existence of the X* phases in W317 is very important. We believe that it is the absence of a tilted phase below the smectic A* phase which is the cause of the reduced temperature dependence of the electroclinic tilt. In a smectic C*–A* material, the electroclinic coefficient increases dramatically as the temperature approaches the smectic C*–A* transition from above [6]. However, in electroclinic materials with non-tilted underlying phases, the electroclinic coefficient levels off over a narrow temperature range at the bottom of the smectic A* phase [10–12]. W317 shows this reduced temperature dependence over a much broader range of about 15°C.

The size of the electroclinic effect in W317 is also puzzling. In smectic C*–A* materials, the electroclinic effect can be maximized by operating at temperatures very close to the smectic C*–A* transition. While this affords large tilt angles, it has the disadvantage of maximizing the temperature dependence of the electroclinic effect. W317 has a large electroclinic effect, but not the accompanying temperature dependence. Therefore, W317 must be very nearly a smectic C* material for changes in

some parameter other than temperature. This class of material was hinted at by Andersson *et al.* [13]. While we have not found this parameter yet, this idea is supported by the fact that slight variations in the molecular structure of W317 result in a dramatic decrease in the size of the electroclinic effect and the appearance of a smectic C* phase.

6. Conclusions

Below its smectic A* phase, W317 has at least three metastable orthogonal phases. While these phases are not yet identified, we believe they are the cause of the reduced temperature dependence of the electroclinic effect in the smectic A* phase. We have demonstrated an electroclinic effect in these phases which is smaller and slower than in the smectic A* phase. Future work will involve identification of the X* phases, and attempts to increase the size of the electroclinic effect by modifying the molecular structure.

This paper represents U.S. Government work and is not protected by U.S. copyright. The authors thank M. D. Wand (Displaytech Inc., Boulder CO) for supplying the W317 samples for these measurements. This work was supported in part by NSF grant DMR8901657 and ARO contract DAAL03-90-G-002.

References

[1] WALBA, D. M., ROS, M. B., SIERRA, T., REGO, J. A., CLARK, N. A., SHAO, R. WAND, M. D., VOHRA, R. T., ARNETT, K. E., and VELSCO, S. P., 1991, *Ferroelectrics*, **121**, 247.
[2] WILLIAMS, P. A., CLARK, N. A., ROS, M. B., WALBA, D. M., and WAND, M. D., 1991, *Ferroelectrics*, **121**, 143.
[3] NISHIYAMA, S., OUCHI, Y., TAKEZOE, H., and FUKADA, A., 1987, *Jap. J. appl. Phys.*, **26**, 153.
[4] LEE, S. D., and PATEL, J. S., 1989, *Appl. Phys. Lett.*, **54**, 1653.
[5] ANDERSSON, G., DAHL, I., KOMITOV, L., MATUSZCZYK, M., LAGERWALL, S. T., SKARP, K., and STEBLER, B., 1991, *Ferroelectrics*, **114**, 137.
[6] ABDULHALIM, I., and MODDEL, G., 1991, *Liq. Crystals*, **9**, 493.
[7] LEE, S. D., and PATEL, J. S., 1989, *Appl. Phys. Lett.*, **55**, 122.
[8] JOHNO, M., CHANDANI, A. D. L., TAKANISHI, Y., OUCHI, Y., TAKAZOE, H., and FUKUDA, A., 1991, *Ferroelectrics*, **114**, 123.
[9] VAN HAAREN, J. A. M. M., and RIKKEN, G. L. J. A., 1989, *Phys. Rev.* A, **40**, 5476.
[10] ANDERSSON, G., DAHL, I., KUCZYNSKI, W., LAGERWALL, S. T., SKARP, K., and STEBLER, B., 1988, *Ferroelectrics*, **84**, 285.
[11] BAHR, CH., and HEPPKE, G., 1988, *Phys. Rev.* A, **37**, 3179.
[12] ETXEBARRIA, J., REMÓN, A., TELLO, M. J., and SERRANO, J. L., 1989, *Liq. Crystals*, **4**, 543.
[13] ANDERSSON, G., DAHL, I., KOMITOV, L., LAGERWALL, S. T., SKARP, K., and STEBLER, B., 1989, *J. appl. Phys.*, **66**, 4983.